Feedback-giving guide wire for vaso-protective use in minimal invasive heart surgery

Nicolas Alexander Kuhn

***Abstract*—As a treatment option for heart valve diseases the conventional open thorax surgery is a common surgical procedure. In the last years less invasive treatment options developed, including the most minimal invasive option named transcatheter aortic valve implantation (TAVI). For this method guide wires are used to preset the path for the catheter carrying the new valve. These guide wires are placed with help of x-ray imaging due to the lack of insight into the artery system from outside. This work focuses on the developement of a sensorized guide wire prototype for catheterization applications. A flex bending sensor wrapped around a guide wire and secured with heat shrink tubes is used as the smart element of this prototype. The developed smart guide wire is tested inside a water flowed tube phantom mimicking a blood vessel with heart beat by a pump operating in pulsatile mode. At different scenarios that are mostly relevant for the clinical surgery, i.e. guide wire with stenosed tube, with heartbeat, without heartbeat and in the simplest case without blood (water). The results show that the sensor can detect all different scenarios inside the phantom and is able to detect angle and force with high accuracy. The outcome of the study is that the developed smart guide wire has potential to support heart valve surgeries in the future.**

***Index Terms*—TAVI, Smart guide wire, Flex bending sensor, ESP32, Experimental analysis of raw sensor data, Force measurement**

I. Introduction

THE surgical treatment of aortic valve diseases splits up into different approaches that can be taken. The decision on which method should be used depends on the health state of the patient [1]. The conventional approach as a treatment option is the full sternotomy [2]. To reduce the invasiveness with consistent efficacy, quality and safety, techniques were developed to reduce the stress given to the body with fully opening the thorax [2]. Another alternative to conventional surgery is the application of the trans catheter aortic valve implantation (TAVI) [3], [4]. For placing a new valve onto the old one, a guide wire is navigated through the artery system, mostly starting from the femoral artery (trans femoral TAVI or TF-TAVI), up to the tip of the heart in the left ventricle [3], [5]. Due to the minimally invasive procedure, medical x-ray imaging is used to detect the guide wires and catheters position and movement inside the vascular system of the patient [6]. This results in radiation exposure for all participants in the surgical theater.

The aim of this work is the development, building and testing of a sensorized guide wire prototype. The requirement, elaborated with a heart surgeon, is the creation of a solution for gathering information out of a tube system mimicking the body of a patient with help of a sensor. The sensor used in this work is a flex bending sensor, which has not been used from other research teams as an attempt. After some first tests, which are needed for the following development of the prototype, the building and further testing will be shown. The final tests of the prototype in the named circuit of tubes with different diameters and a pump will be performed with water and a constant applied force to simulate the circumstances closest to reality.

This paper summarizes the content of the masters thesis for the masters conference [7].

Nicolas Alexander Kuhn is with the Department of Medical and Health Technologies, MCI, Innsbruck, Austria, e-mail: n.kuhn@mci4me.at.

II. Materials and Methods

In this paper only the requirements and the building of Prototype 2 is shown, although there was a first, not working, attempt.

A. Materials

1) Requirements: The smart guide wire should be able to detect and show the changes in the measured values when the wire has contact to the tubes wall or an occlusion inside the patients vessel. Additionally the observation of a value change when the wire is approaching a bottleneck inside the tubes and how it behaves after passing it is of interest. Based on the measured values it can then be said in which environmental condition the guide wire is at the moment and if further investigations are needed to receive sufficient information. Due to the sensitivity of the sensor even small changes in pressure or friction should be made visible.

2) Developement of the Prototype: It was build out of one guide wire, a flex bending sensor, wires and a mixture of hot glue and heat shrink tubes to make the electrical parts resistant to water. The flex bending sensor was glued to the guide wire with hot glue. It was positioned directly behind the floppy area at the tip of the original guide wire. This bases on the assumption, that the floppy tip would not be able to damage the vascular wall due to its mechanical properties. The calculations and collection of data with the micro controller will be explained in Section II-B2. The operation area of the guide wire would be later in the vascular system or, was in this case for testing, inside a tube system filled with water. To keep connection to the sensor at the tip of the guide wire, which will be inside the tube system, cables must be connected to the connection pins of the sensor itself. These were soldered to the pins and additionally fixed with help of heat shrink tubes. Each one of the connections was secured with one heat shrink tube and in addition a bigger one holding the construction in place. The cables were wrapped parallel around the wire to

keep the diameter as small as possible and ensure stability of the construction. The wire was cabled over a length of 130 cm, with the first 7 cm in Prototype 2, occupied by the sensor, to enable a sufficient operation range inside the tube system for testing. It was needed to ensure a connection to the breadboard used for the data readout. Therefore at the end of the cables metal pins were attached to enable that connection. These did not enter the testing circuit and thus did not come into contact with water. To make the electrical components and connections watertight, the complete prototype, from the end of the sensor at the connection points to the end of the wiring around the wire, was covered with a combination of heat shrink tubes and hot glue. The connections between the 200 mm long heat shrink tubes were stabilized with hot glue to prevent slipping and water intrusion. The tip of the wrapped sensor was sealed as well with a thin layer of hot glue. This ensures persistent functionality of the data capturing and the use of this prototype itself.

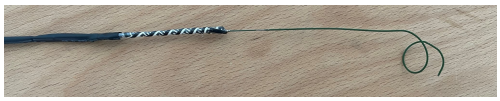

Fig. 1: Prototype 2

TABLE I: Parts of the testing circuit with numbers

Number	Component
1	Sensorized guide wire prototype
2	Square timber with different diverter pulleys
3	Clothespin with weights
4	Reservoir
5	Tube holder for the reservoir
6	Water pump
7	Tube holder for the mounting plate
8	Clamp to change the diameter of the tubes
9	Mounting plate
10	Tubes for testing the prototype

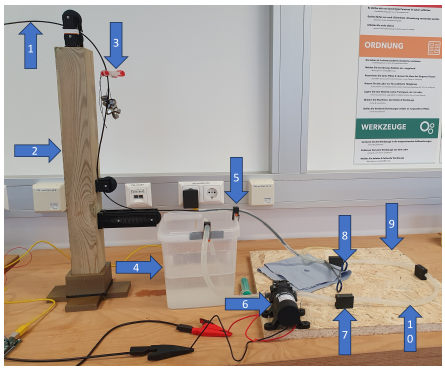

Fig. 2: Structure of the test circuit during the experiments

B. Methods

1) Testing Circuit: The testing circuit was build from silicon tubes of different diameters, where water was pumped through with the water pump. The water was as well useful to prevent high friction forces of the wire inside the tubes.
For the testing circuit different parts have been designed and 3D-printed to fixate and guide the tubes. These were mounted onto a wooden board to hold the tubes in place. A roll was designed with two holders to guide the guide wire into the tube system. From these, two were stacked on top of each other to prevent the guide wire from slipping out of the guidance. They were mounted on top of a 7 cm times 7 cm wooden square timber. For the square timber a mounting foot was designed as well to make it stand stable. Additionally, holders and wheels were designed that acted as a diverter pulley. These, with different lengths, were mounted at the side of the square timber. With this arrangement it was possible to put weights onto the angled wire. Yarn and a clothespin were used to attach the weight to the wire pushing it into the tube system by the created force. To make this possible nuts were used. They could be attached and the weight changed easily. With this it was tried to make the results resilient and as well repeatable and comparable. The holders for the tubes at the reservoir were as well designed in Inventor and supported the stability of the testing circuit.
The pump was positioned at the end of the circuit with a tube reaching into the water inside the reservoir. Table I shows the parts of the testing circuit numbered from 1 to 10, which is shown as an image in Figure 2.

2) Arduino IDE Code and Formulas for the Force Measurement: To make the measurements possible, some coding must be done to read out the data from the sensor with the micro controller. Therefore the program Arduino IDE was used and the code then transmitted to the micro controller. The gathering of data was done with an ESP32 and the operation control with an Arduino UNO, with which a rectangular shaped output signal was created to generate pulsatile flow with the pump. To calculate a force out of the gathered data, it was assumed that the force distribution is similar to the support reactions of a beam fixed at one side with a force affecting the loose end. The corresponding equation to that is shown in Equation 1 [8].

$$\alpha = \frac{F \cdot l^2}{2 \cdot E \cdot I} \tag{1}$$

With the bending angle α in rad, the force F in N, the length of the bar l in mm, the Young's modulus E in N/mm^2 and the area moment of inertia I in mm^4. The values of E for the wire was taken out of literature [8]. The area moment of inertia was calculated with the following Equation 2. In this case the equation for the axial surface moment of inertia was used because it describes the stiffness against bending in axial directions [9].

$$I = \frac{\pi \cdot r^4}{4} \tag{2}$$

With the mathematical constant π and the radius r in mm. To find the bending angle, which was essential for this calculation, the characteristic curve of the sensor was recorded, relating the angle to the value measured by the sensor. This had to be done after the prototype was build, because the values at rest were different when the sensor is attached to the wire. From the angle calculated with the formula of the characteristics curve, the force acting on the wire can be calculated. Equation 1 must be converted to the force F and the angle from degrees to radiant. The conversion of the angle from degree to

radian measure is shown in Equation 3, with the mathematical constant π and the angle in degrees that must be inserted as the variable x. Equation 4 shows the formula to calculate the force, with the same variables as in Equation 1.

$$x\ ^\circ = x \cdot \frac{\pi}{180}\ rad \tag{3}$$

$$F = \frac{2 \cdot E \cdot I \cdot \alpha}{l^2} \tag{4}$$

3) Experimental Design and Measurements: The tests done with the raw sensor and Prototype 1 are shown in the complete masters thesis. For this paper only the results of the working Prototype 2 are shown. The experiments with Prototype 2 have been done in four parts. Firstly the bit values to corresponding bending angles were collected. Therefore the sensor was bend to a certain angle and the values collected for 20 seconds. From the data points the mean value was calculated. Afterwards the testing of the prototype was done outside the circuit to measure the weight at the tip of the wire when weight was attached to it. Therefore a scale was glued to the wall and the tip of the wire placed in the middle of it. The scale´s plate was optimized with a piece of double-sided adhesive tape to prevent the tip from slipping. After that the experiments have taken place in the above named testing circuit. The wire was placed inside it and different measurements were done without and with water. The following list shows the experiments and their specifications with a short description of the procedure.

1) Characteristics curve value gathering
   a) 0° bending angle
   b) 5° bending angle
   c) 10° bending angle
   d) 15° bending angle
   e) 20° bending angle
   f) 25° bending angle
2) Outside the Circuit and without water, a scale is placed at the contact point of the wire to the wall
   a) 84.1 g were attached to the wire, weight at tip was measured
   b) 45.1 g were attached to the wire, weight at tip was measured
   c) 25.8 g were attached to the wire, weight at tip was measured
3) Inside the Circuit and without water, 84,1 g were attached to the wire
   a) Sensor was inside the tubes
   b) A clamp was positioned in front of the wire´s tip and closed the tube
   c) Partly closed tube with the sensor positioned at the bottleneck
   d) The clamp was poisitioned directly on the sensor
   e) The sensor was placed at the entrance of the smallest tube
   f) Sensor value outside the tubes and without weight (as reference)
4) Inside the Circuit and with water, 84,1 g were attached to the wire, pump operated at 6 V 2 A
   a) Value at rest inside water, with weight, pump turned off
   b) Tip of the wire was placed at the entrance of the small tube, without weight, pulsatile flow
   c) Tip of the wire was placed at the entrance of the small tube, with weight, pulsatile flow
   d) Tip of the wire was placed behind the entrance of the small tube, with weight, pulsatile flow
   e) Tip of the wire was placed behind the entrance of the small tube and the tube was party closed with a clamp, with weight, pulsatile flow
   f) Value inside water, with weight, pulsatile flow
   g) Started without clamp, then clamped the tube (in flow direction in front of the sensor), with weights, pulsatile flow
   h) Started without clamp, then clamped the tube (in flow direction behind the sensor), with weights, pulsatile flow
   i) Value inside water, with weight, continuous flow
   j) Started without clamp, then clamped the tube (in flow direction in front of the sensor), with weights, continuous flow

At the end the calculations for the force measurement were done with the results from experiment two, explained in the list above, and the assumed formulas described in Section II-B2.

III. Results

A. Prototype 2

1) Test series one - Values for the characteristics curve: Firstly a characteristics curve of the sensor wrapped around the guide wire was done. The measured bit values without an unit (x-axis) for each defined angle in degrees (y-axis) are shown in Figure 3. The exact values are as well shown in Table II.

TABLE II: Values for the characteristics curve

Bending Angle (°)	Bit Value (-)
0	1834.7
5	1810.2
10	1805.9
15	1772.5
20	1762.8
25	1714.5

With a linear trendline the following Equation 5 was calculated.

$$y = -0.2123 \cdot x + 391.06 \tag{5}$$

The equation can be used to calculate an angle in degrees (y) with a bit value inserted as a x value. To simplify the understanding of the equation it can as well be written as shown in Equation 6.

$$Angle\ in\ degrees = -0.2123 \cdot Bit\ value + 391.06 \tag{6}$$

This was used for the force calculation which results are shown in Section III-A5.

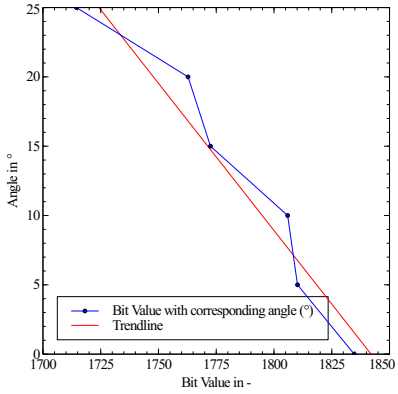

Fig. 3: Values for the characteristics curve with the visualization of the calculated trendline

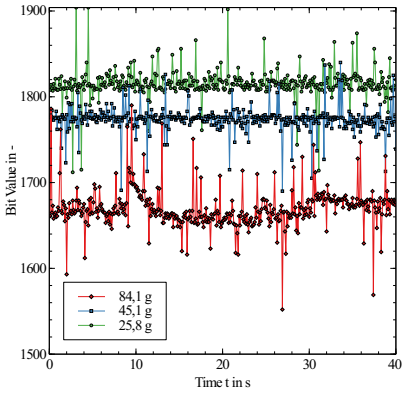

Fig. 4: The sensor values during the test series two to find out how much force is measurable at the tip

2) Test series two - Different weights were applied to the wire and the weight at tip was measured: Table III shows the corresponding weights measured at the tip of the sensor with the different weights applied at the wire. With 84.1 g applied 40.1 g were measured at the tip, with 45.1 g at the wire 29.4 g at the tip and with 25.8 g at the wire 20.5 g at the tip. For the highest weight at the wire almost only half the weight was applied to the tip. The weight at the tip for the two other measurements is as well lower, but only one third less for 45.1 g and one fifth less for 25.8 g.

TABLE III: The weights applied to the wire with the corresponding measured weights at the tip of the wire

Weight applied to the wire	Weight measured at the tip
81.1 g	40.1 g
45.1 g	29.4 g
25.8 g	20.5 g

Figure 4 shows the measured bit values of the experiment, with the time t in seconds on the x-axis and the bit value without an unit on the y-axis. The Figure includes the three measurements with different applied weights to the wire. Shown are 84.1 g in red with diamond shaped data points, 45.1 g in blue with square shaped data points and 25.8 g in green with circular shaped data points. The highest weight applied to the wire shows the lowest measured values and the lowest weight results in the highest measured values.

3) Test series three - Measurements without water inside the tube system: The experiments without water would not have been possible without additional lubrication inside the tubes. The tubes material in combination with the wire and the heat shrink tubes made it impossible to push the wire forward into the tube. Therefore a lubricant from the company WD40 was used to overcome this problem by spraying it into the tubes.
Figure 5 shows the results of the measurements without water inside the tube system with the time t in seconds on the x-axis and the bit values without an unit on the y-axis. The results are named like in the experiments list from Section II-B3. The experiments a (old) (red circles in the Figure) and b (old) (blue diamonds in the Figure) are named like this because the sensor detached during the observation of these experiments. Nevertheless, these two graphs show the results of the sensor inside the tubes with weight applied to the wire (a (old)) and with a clamp positioned in front of the wires tip (b (old)), which values are higher than the one from experiment a (old). Seen in total, the graphs of a (old) and b (old) have the lowest values of this test series.
After the sensor was glued again to the wire, the experiments b (new) to f (pink rectangles in the Figure) were performed, whereby graph f (value at air outside the tube system) was done only as a reference to see the difference between inside and outside the tube system. In Figure 5 it shows the highest values. Below it the measured data of experiment e (the sensor placed at the entrance of the smallest tube, displayed in brown stars) are shown with values around 2400. The graph for experiment b (new) (green squares in the Figure) in the middle of Figure 5 shows values around 2100. The values of the experiments c (partly closed tube with the sensor positioned at the bottleneck, shown as purple crosses in the Figure) and d (clamp is positioned directly onto the sensor, displayed in orange plusses) vary in the course of the measurements. The values of experiment c start at around 1950 and rise slowly above the values of experiment b, with a peak of approximately 2300 at 10 seconds passed, then falling back to values around 2150 until the end of the observation. In experiment d the beginning is reversed in comparison to experiment c. It starts at a value around 2100, falls then to a value of nearly 1950 and evens out at a value of approximately 2000.

4) Test series four - Measurements with water inside the tube system: For the fourth test series many measurements were made, for what reason a Figure including all the graphs as an overview with raw data, like in Figure 5, is not possible. Instead of one Figure with all the experiments, different measurements to be compared are combined into the following graphs, which all show the time t in seconds on the x-axis and the bit values without an unit on the y-axis. At the end of this Section (III-A3) a Figure with all the data is shown and explained, but only containing calculated means.
Figure 6 shows the observations of the experiments with the wire inside the tube system without any clamps and with

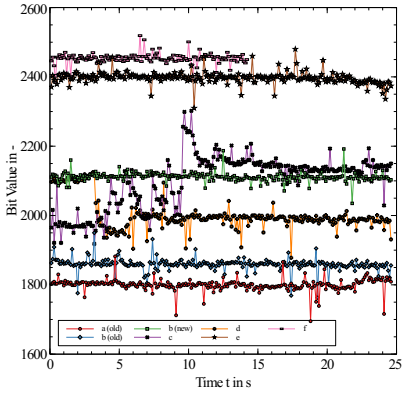

Fig. 5: All the measurements without water inside the tube system

different conditions of the pump. Graph a (red circles) shows the bit values over time inside water with the pump turned off. Graphs f (blue triangles) and i (green rectangles) show the values with the pump turned on in different modes. In f the pump worked in pulsatile mode and in i without the additional electrical circuit in continuous flow. Graph i has a wave form with a high amplitude, peaks up to values of 3000 and a nearly uniform run. In graph f the pulastile mode is identifiable with values lower than the curve i. It has sharper peaks and a lower amplitude. Graph a shows the lowest values over time that fluctuate around 2600.

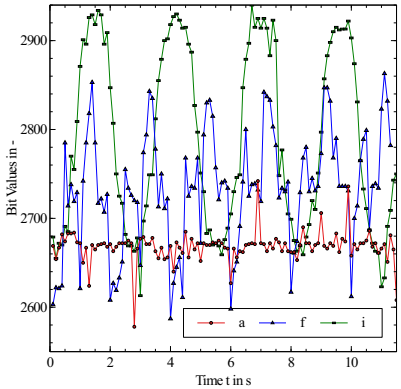

Fig. 6: Graphic illustration of the experiments a (values inside water with the pump switched off), f (values inside water with the pump operating in pulsatile mode) and i (values inside water with the pump operating in continuous mode)

In Figure 7 the experiment results of the wires tip placed at the entrance to the small tube without weight (b, red diamonds) and with weight (c, blue squares) are shown. While the graph of b is consistently showing the fluctuations expected from the pulsatile flow, the graph of experiment c starts at a similar sensor value and a similar amplitude but changes shape over time. At around 13 seconds the amplitude and the overall bit value decreases. Figure 8 displays the results of the experiment with the tip of the wire behind the entrance of the small tube (d, red crosses) and at the same position with a clamp decreasing the tubes diameter (e, blue stars), both

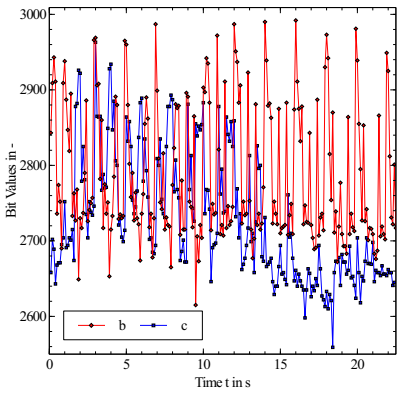

Fig. 7: Results of the experiments b (the wires tip placed at the entrance to the small tube without weight) and c (at the same position with weight)

with pulsatile flow. In both graphs the fluctuation due to the pulsatile flow is recognizable. The graph of experiment e has lower bit values than the values observed in experiment d. The highest peak values in e are at around 2650 and in d at around 2715.

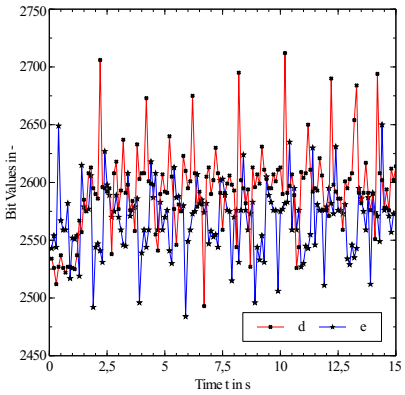

Fig. 8: Results of the experiments d (the tip of the wire behind the entrance of the small tube) and e (at the same position with a clamp decreasing the tubes diameter)

The results of the experiments with clamping the tube in the course of the measurement are shown in Figure 9. The red curve with triangles (g) show the results of clamping the tube in flow direction in front of the sensor and the blue curve with diamonds (h) the results of clamping the tube in flow direction behind the sensor. In graph g the tube gets clamped at approximately 12.5 seconds, resulting in a decrease of amplitude and overall lower values than at the beginning of the measurement. In graph h the tube gets clamped slightly later at around 13 seconds. Due to a blockage of the tube with the clamp the peaks arised. The graphs distinctive peak downwards reaches a value of around 2425 before shooting nearly straight up to 3425. After rearranging the clamp, to restore the flow, the values settled with the expected fluctuations due to the pulsatile flow. The overall values of this curve are higher then at the beginning.

Interesting is as well the difference between the results of

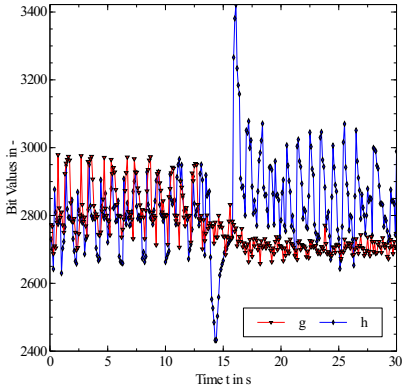

Fig. 9: Results of the experiments g (clamping the tube in flow direction in front of the sensor) and h (clamping the tube in flow direction behind the sensor)

clamping the tube with different operation modes of the pump, which is shown in Figure 10. Here, the measurements from experiment g (red triangles) are compared with the results of experiment j (blue stars), where the tube is clamped as well in course of the measurement, but with the pump working in continuous flow mode. Graph g is the same as in the previous Figure 9. Graph j shows a clamping of the tube at around 10 seconds with a reduction of the amplitude. Compared, the amplitude does not change as much as seen in graph g. Neither is a severe overall lowering of the bit value visible.

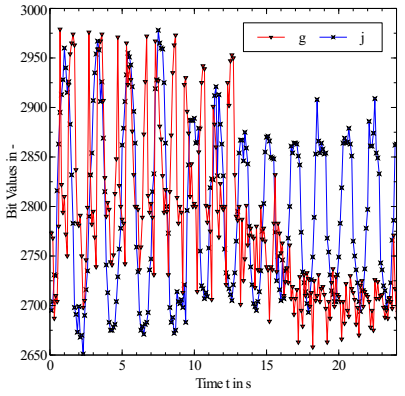

Fig. 10: Results of the experiments g (the clamped tube in flow direction in front of the sensor in pulsatile flow) and j (the clamped tube in flow direction in front of the sensor in continuous flow)

Figure 11 shows the initially mentioned means of all experiments made for this test series. Most of the experiments stayed the same, with repeating patterns, over time and are therefore displayed as straight lines. This applies to the measurements a, b, d, e, f and i. The other measurements like c, g, h and j, changed more severely over time, with changing patterns, why they are shown a bit differently. Different sections in these results are chosen to show the course of the original graph. One exception is the graph of experiment h, where for the extreme peaks to the bottom and to the top the values from the original measurements are taken.

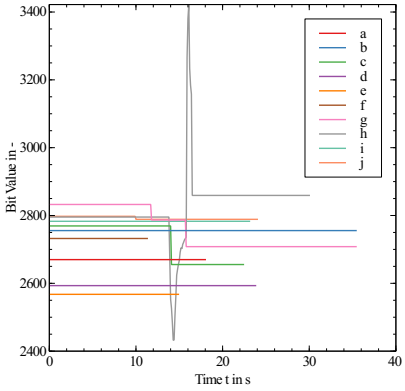

Fig. 11: Calculated means of each experiment, some are split up into small sections

5) Force calculation with Prototype 2: With the characteristics curve from Section III-A1 and the means of the results from Section III-A2, the applicability of the force calculation can be done. The results from Section III-A2 were chosen, because the force at the tip could be calculated due to the measured weights at the tip. Additionally it was assumed, that the tip was pushed into the scale with earths acceleration 9.81 m/s^2. The values for inertia I were calculated with Equation 2 and a radius r of 0.445 mm. The angle that resulted from the calculation with Equation 5 were converted from degrees into radiant with Equation 3. The values for the calculation are shown in Table IV, except for I (0.03 mm^4), E (210 000 N/mm^2) and l (70 mm), which are the same for all calculations.

TABLE IV: Values for the force calculation

Weight at wire (g)	Weight at tip (g)	Mean Bit Value	α (°)	α (rad)
84.1	40.1	1669.75	36.57	0.64
45.1	29.4	1773.69	14.51	0.25
25.8	20.5	1815.41	5.65	0.099

With the given values from Table IV and the approximation Equation 4, the value for the force at the tip could be calculated. The results of the calculations are shown in Table V, where the weights at the tip, the expected force which the tip applies to the scale and the calculated force with the approximation equation are shown. The expected value differs from the calculated force most with the highest weight at the tip. Here it is nearly four times more with the approx. formula (1.65 N) than the expected value (0.39 N). Reducing the weight at the tip decreases as well the differences between the expected and calculated values. With 29.4 g at the tip the expected value is 0.29 N and a calculated value of 0.64 N nearly double the value. The closest of values to the expected (0.20 N) is in the experiment with 20.5 g at the tip and a calculated value of 0.26 N.

IV. Discussion

A. Prototype 2

Prototype 2 was build after Prototype 1 failed due to technical problems. Prototype 2 which was used for the experiments,

TABLE V: Calculated Forces with the corresponding weights at the tip

Weight at tip (g)	$F_N = m \cdot a$ (N)	Force calculated with approximation formula (N)
40.1	0.39	1.65
29.4	0.29	0.64
20.5	0.20	0.26

also has some small errors that have occured during the first tests. It turned out that the sensor gave different, higher or lower, values depending on the direction it was bent in. If the sensor was bent into only one direction, the results still were consistent and repeatable. As it is not predictable in which direction the wire bends, this is the greatest limitation of this project. This could be attributable to the wrapping of the sensor. The sensitivity of the sensor to external pressure was not affected by that. Like in Prototype 1 hot glue was used to fixate the sensor to the wire. Moreover it turned out that this glue was stable in short term, but shows weaknesses in the long term, because the sensor has come lose after some time. However, the loosening could also have been favored by the high temperatures inside the laboratory. Knowing that, the first two experiments outside the tube system were performed with increased attention to ensuring that the sensor bends in only one, consistent, direction.

1) Test series one: The characteristics curve from the first test series showed a nearly linear relationship between the bit value and angle, although the original relationship was non-linear. This change in properties is explainable with the wrapping of the sensor.

2) Test series two: In this test series it was tried to show a value change from the sensor with different weights applied to it, with the additional focus on the weight that was measureable at the tip. It stands out that the measured weight differences at the tip changed depending on the weight hanging on the wire. This can be explained with the setup of the experiment. Hanging weight onto the wire induced a bending behind the first diverter pulley. This resulted in contact of the wire with the square timber and thus also in a lower weight at the tip.

After these experiments a weight for the following investigations was chosen. In an experiment done by [10] the applied force increased over time due to the distance traveled inside the phantom. The measurements were done in a range from 0 N to approximately 2.5 N of force pushing the guide wire into the phantom [10]. Additionally to that information, a test was done with the experimental setup described in this work. The tip of the guide wire was carefully pressed against the scale in an attempt to obtain an approximate estimate of how much weight is applied to the tip when pushed very carefully. Based on the result and the gathered information, it was decided to use the weight of 84.1 g attached to the wire, althought at this weight the largest deviation between attached weight and measured weight at the tip was found. Friction and loss of force due to other contact points also had to be considered, which underlined the choice of the largest weight.

3) Test series three: During the experiments without water inside the tube system WD40 was used to make the insertion of the prototype into the tubes possible. One weakness of the hot glue that was used in this work is the potential influence of heat to the stability. Another could be the resistance against the lubricant from WD40 that had to be used. After the first test (a (old)) the sensor started to detach, which is visible in the results of experiment b (old). Lower values would have been expected, but the results show higher ones. The sensor had to be glued again, which changed the resulting values for the rest of the experiments to be higher. The data for graph f was observed with the newly glued sensor as a reference to compare the values of the sensor inside the tube system with the value from outside. The significant differences were clearly visualized.

The only experiments delivering unexpected results were c and d. The value change in experiment c is hard to explain. The values should be similar to the ones from experiment b (new), like they are at the end of the recording, but they start at a very low point. The explanation for the value drop in experiment c could be the late application of the clamp to the tube and the sensor. Concluding the experiments, in disregard of experiment a (old) and b (old) and with the explanations above, the results suit the expectations. The lowest values in experiment c (highest pressure) and the increasing values for different positions and circumstances with or without a clamp have been shown decently.

4) Test series four: The most realistic experiments were performed in the fourth test series with water inside the tube system. Some experiments developed out of an interview with Dr. Nikolaos Bonaros, who gave interesting input and incentives for the development of meaningful experiments close to a realistic situation. Inspecting the measurements under different conditions of the pump mode without clamps, it showed interesting, unexpected courses of the graphs. The pump working in continuous mode created, as well as it working in pulsatile mode, repeating peaks up and down. This result was expected for the pulsatile mode, but surprising for the results from the continuous flow. It can be explained with the inner structure of the pump and the way of it creating flow. As the pump is a dual chamber membrane pump that alternating pushes water out of the chambers. Like this a continuous like flow is created.

The results of experiment c that is compared to experiment b in Figure 7 had an unclear course. A possible explanation could be that the weight was applied after the measurment started. As the position of both measurements is exactly the same, this is the most logical explanation. The force, applied by the weight, then pushes the sensor into the tubes wall, which causes a reduction in amplitude and increases the pressure measured by the sensor.

The changes in graph d to e result from the positioning of a clamp that reduced the tubes diameter and therefore as well changed the speed of water flowing through the area of decreased diameter. This caused the pressure to reduce in the narrow area and increase again when the diameter was back to normal. The area in flow direction behind the bottleneck showed higher pressure what can be explained with a change of flow pattern. Due to the higher velocity and the blockage the flow pattern becomes more turbulent what results in the named

increase of pressure. Additionally increases the decelerating of the water the pressure, which can be named as a reason as well. The same is visible in graph g and can be explained with the same phenomenon like the changes in graph e. The idea for measurement g was given by the heart surgeon, for whom it was interesting to know if the sensor is able to detect changes appearing in the tube while measuring. This should simulate the real environment, when the guide wire approaches and passes a point with a narrowed diameter inside the vessel. The approaching is shown in graph g and the passing is shown by graph h. The lower pressure in front of the bottleneck (graph h) can be explained with a more sorted flow pattern at this position. The peaks of graph h can be explained with the clamp completely blocking the tube. The pressure rised straightly (measured values decreased) and the pump stopped operating, why the measured values nearly instantly jumped upwards. The quick change of the clamps position made the pump work again.

The flow mode affected the measurements as well. The comparison between graph g and j also was proposed by the cardiac surgeon. The flow mode affected the pressure causing a decrease in both graphs, but with less changes in the continuous flow graph.

The graph with the mean values was created to give an overview on the measured pressure differences at the different positions inside the tubes and the use of a clamp. The lowest values of d and e can be explained with the position inside the tube system. These two measurements were made deepest into the tube, which could have caused the pressure difference. The different lengths of the graphs are due to the fact that in some measurements no changes could have been observed over time, and the data capturing was therefore stopped.

5) Force measurement: The formula for the force calculation was assumed to come close to reality and to try if a force measurement with the build prototype can be implementable. As the results show, the outcome is highly dependent on the characteristics curve of the sensor. Bit values exceeding the included ones make the calculation unrealistic. With values being in range of the characteristics curve at least a narrowing of the forces acting at the tip of the sensor was possible. The calculated force with the lowest weight measured at the tip varied only very weakly from the expected value. So it can be assumed that the approximation formula used in this work is suitable for low forces and bending angles, but that was not sufficiently tested. Additionally the other sensitivity of the sensor must be included, as it reacts quite sensitive to pressure. As a guide wire is used in the vascular system of humans, where liquids create pressure differences, this formula is not suitable anymore. To have a reliable force measurement inside liquids both methods, the calculation of force by external pressure and the bending of the wire, must be combined. This was not done in this work, as the main focus was laying on the identification of appearing differences of the sensor values, which already give a good impression on changes from environmental differences. It must be added that the Young's modulus is only assumed to be right as well. From this perspective additional measurements to find out the exact value and specify the calculations could be done as well.

V. Conclusion

This work showed the successfull development of a sensorized guide wire for minimal invasive heart surgery using a flex bending sensor. The different experiments outside the tube system, inside the tube system without water and inside the tubes with water gave a good insight into the working principle of the sensor used in this work. The approach of wrapping the sensor was, despite the failure of the first Prototype, a working idea. This approach still had some small defects, but was able to detect changes in the situations named by Dr. Nikolaos Bonaros. Approaching a bottleneck could be made visible as well when the sensor had passed this narrowed area. At different positions inside the tubes, different heights of values were measured, which lead to the assumption that different pressures appear depending on the position inside the tube. The testing circuit used for the experiments worked as intended. It had some definable limitations which, if once defined, could be excluded as a source of error. For future work, a smaller, more narrow, version of this kind of sensor could be used to reduce the effects caused by the wrapping of the sensor around the wire.

The formula used for the force calculation was assumed to be applicable for this field. This could not be proven completely but based on the results, it can be concluded that the formula works better for smaller forces and bending angles. This could be optimized in future works together with the consideration of the pressure forces acting on the sensor inside a liquid. The exact values for the Young's modulus could be determined for further work as well to receive more precise results.

References

[1] B. R. Linfman, M.-A. Clavel, P. Mathieu *et al.*, "Calcific aortic stenosis," *Nature Reviews Disease Primers*, vol. 2, no. 16006, pp. 1–64, 2016.

[2] M. Glauber, M. Ferrarini, and A. Miceli, "Minimally invasive aortic valve surgery: state of the art and future directions," *Annals of Cardiothoracic Surgery*, vol. 4, no. 1, pp. 26–32, 2015.

[3] R. Cocchieri, R. Petzina, M. Romano, D. Jagielak, N. Bonaros, M. Aiello *et al.*, "Outcomes after transaortic transcatheter aortic valve implantation: longterm findings from the european route," *European Journal of Cardio-Thoracic Surgery*, vol. 55, pp. 737–743, 2019.

[4] G. C. M. Siontis, P. Overtchouk, T. J. Cahill *et al.*, "Transcatheter aortic valve implantation vs. surgical aortic valve replacement for treatment of symptomatic severe aortic stenosis: an updated meta-analysis," *European Heart Journal*, vol. 40, pp. 3143–3153, 2019.

[5] B. Clayton, G. Morgan-Hughes, and C. Roobottom, "Transcatheter aortic valve insertion (tavi): a review," *The British journal of radiology*, vol. 87, no. 1033, p. 20130595, 2014.

[6] S. Sehatzadeh, B. Doble, F. Xie, G. Blackhouse, K. Campbell, K. Kaulback, K. Chandra, and R. Goeree, "Transcatheter aortic valve implantation (tavi) for treatment of aortic valve stenosis: An evidence-based analysis (part b)," *Ontario Health Technology Assessment Series*, vol. 12, no. 14, pp. 1–62, 2012.

[7] N. A. Kuhn, "Feedback-giving guide wire for vaso-protective use in minimal invasive heart surgery," Master's thesis, Management Center Innsbruck, Innsbruck, 2023.

[8] D. Gross, W. Ehlers, P. Wriggers, J. Schröder, and R. Müller, *Formeln und Aufgaben zur Technischen Mechanik 2*. Berlin, Germany: Springer, 2017, vol. 12.

[9] W. Hauger, C. Krempaszky, W. A. Wall, and E. Werner, *Formeln und Aufgaben zur Technischen Mechanik 2*. Berlin, Germany: Springer, 2017, vol. 9.

[10] N. Koev, "Entwurf, präparation und charakterisierung von führungsdrähten mit integriertem silizium-mikro-kraftsensor für die herzkranzgefäß-katheterisierung," Ph.D. dissertation, Dissertation, Darmstadt, Technische Universität Darmstadt, 2021.